2009 American Control Conference
Hyatt Regency Riverfront, St. Louis, MO, USA
June 10-12, 2009

An Adaptive Observer Design for Recirculation based Solid Oxide Fuel Cell Systems using Cell Voltage Measurement

Tuhin Das

Abstract— **In this paper we present an observer design for species concentration estimation in recirculation based solid oxide fuel cell systems. The proposed strategy is useful for sensor reduction and control. In designing the observer, we attempt to reduce the number of required concentration sensors, that are often less reliable and also expensive, and instead use readily available voltage. We design a nonlinear adaptive observer based on voltage measurement that is an improvement upon our prior results. For this observer, we prove ultimate boundedness of state and parameter estimation errors with arbitrarily small error bounds.**

I. NOMENCLATURE

F	Faraday's constant, 96485.34 *Coul./mol*
i	Current draw, *A*
k	Anode recirculation fraction
MW	Molecular weight, *kg/mol*
$\dot{M}_{in}$	Anode inlet mass flow rate, *kg/s*
$\dot{M}_o$	Anode exit mass flow rate, *kg/s*
N	Number of moles, *moles*
$\dot{N}_{air}$	Molar flow rate of air, *moles/s*
$\dot{N}_f$	Molar flow rate of fuel, *moles/s*
$\dot{N}_{in}$	Anode inlet flow rate, *moles/s*
$\dot{N}_o$	Anode exit flow rate, *moles/s*
n	Number of electrons participating in electro-chemical reaction, $(= 2)$
P	Pressure, Pa
R_u	Universal Gas Constant, 8.314 *J/mol/K*
r_I, r_{II}, r_{III}	Rates of reforming reactions, *moles/s*
r_e	Rate of electrochemical reaction, *moles/s*
T	Temperature, *K*
V	Volume, m^3
V_{cell}	Cell voltage, $volt$
$\mathcal{N}_{cell}$	Number of cells
$\dot{\zeta}$	Molar flow rate, *moles/s*
$\mathcal{R}$	Species rate of formation, *moles/s*
$\mathcal{X}$	Species mole fraction
Subscripts	
a	Anode control volume
ex	Exit condition of control volume
g	Generic gas control volume
in	Inlet condition of control volume
i, j	Values of 1 - 7 represent species CH_4, CO, CO_2, H_2, H_2O, N_2, and O_2
r	Reformate control volume
ss	Steady-state

Tuhin Das is an assistant professor of Mechanical Engineering at Rochester Inst. of Tech., 76 Lomb Memorial Drive, Rochester, NY 14623, tkdeme@rit.edu

II. INTRODUCTION

In recent years Solid Oxide Fuel Cells (SOFC) have attracted interests due to factors such as their fuel flexibility and tolerance to impurities. High temperature operating conditions (800 to 1000°C) of SOFCs are conducive to internal reforming of fuels and the exhaust gases are excellent means for sustaining on-board fuel reforming. SOFCs are not only tolerant to carbon monoxide but can also use it as fuel. Furthermore, high operating temperatures makes SOFC-Gas Turbine hybrids excellent combined heat and power (CHP) systems. Optimal performance of SOFC systems can be realized through well designed control strategies. Critical performance variables such as fuel utilization and steam-to-carbon-ratio (STCR) play important roles in determining the overall efficiency and longevity of the system [11], [5]. Hence they must be controlled within safety limits during operation.

Utilization and STCR are functions of species concentrations. Hence, for implementing control algorithms, it is necessary to measure the concentrations. The reforming process in SOFCs results in a number of gaseous species in the reformer and the fuel cell. For instance, steam reforming of methane results in five species namely, CH_4, CO, CO_2, H_2 and H_2O. Control of utilization and STCR would therefore require a large number of concentration sensors which would elevate costs and complicate the hardware. A means of reducing concentration sensors is to design observers that dynamically estimate the species concentrations. In this paper, we design an observer for a steam reformer based tubular SOFC system with anode recirculation and methane as fuel. We develop a lumped control-oriented model that captures the details of heat and mass transfer, chemical kinetics and electro-chemical phenomena of the system. Detailed description of this model can be found in [3].

In the literature there are few observer designs for fuel cell systems, [1], with existing designs focusing on either chemical reactors or on fuel cells exclusively. In contrast, we consider a coupled steam reformer and fuel cell system. The observers in [6] and [8] rely on temperature dynamics. In our observer design, we refrain from using the temperature dynamics of the SOFC system. This is because high temperature operating conditions can result in significant heat exchange through radiative means or otherwise, which would remain unmodeled. Several designs such as [8] and [13] assume prior knowledge of reaction rates. However, in [4] the author shows estimation errors arising from uncertain reaction rate parameters and adopts an adaptive approach to

978-1-4244-4524-0/09/$25.00 ©2009 AACC

circumvent this issue. In [6], the observer design is based on coordinate transformations that eliminate reaction rate terms. In our adaptive design, we treat the rates of steam reforming reactions as unknown parameters that must be dynamically estimated. In [1], the authors have designed an adaptive observer for hydrogen estimation in a Polymer Electrolyte Membrane (PEM) fuel cell. The observer considers the inlet hydrogen partial pressure as a slowly varying unknown parameter and uses voltage measurements.

This paper is organized as follows. In the next two sections we describe the SOFC system and provide an outline of the system model. Next we present the problem and summarize our prior results. We then present the proposed dynamic observer design that uses cell voltage measurements. We prove the boundedness and convergence properties of the observer followed by simulation results. Finally, we provide the concluding remarks.

III. SYSTEM OVERVIEW

Our analysis is based on a steam reformer based tubular SOFC system. The system consists of three primary components, namely, the steam reformer which produces a hydrogen-rich gas from a mixture of methane and steam, the solid oxide fuel cell which generates electricty from electrochemical reactions, and the combustor where excess fuel is burnt to generate heat. Methane is chosen as the fuel for the system, with a molar flow rate of $\dot{N}_f$. It is noted here that the analysis and control development approach can be extended to other fuels as well, such as methanol, ethanol, etc. The SOFC system is described in Fig.1.

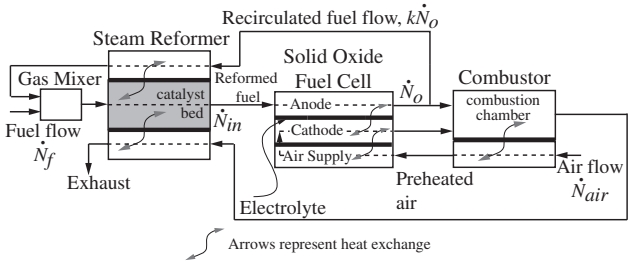

Fig. 1. Schematic diagram of the SOFC system

The reformer produces a hydrogen-rich gas which is supplied to the anode of the fuel cell. Electrochemical reactions occuring at the anode due to current draw results in a steam-rich gas mixture at the anode exit. A fraction k of the anode efflux is recirculated through the reformer into a mixing chamber where fuel is added. The recirculation k is assumed to a fixed known fraction. In tubular SOFCs, recirculation is typically achieved through the deliberate use of imperfect seals. The mixing of the two fluid streams and pressurization is achieved in the gas mixer using an ejector or a recirculating fuel pump, [5]. The steam reforming process occuring in the reformer catalyst bed is an endothermic process. The energy required to sustain the process is supplied from two sources, namely, the combustor efflux that is passed through the reformer, and the aforementioned recirculated anode flow, as shown in Fig.1. The remaining anode efflux is mixed with the cathode efflux in the combustion chamber. The combustor also serves to preheat the cathode air which has a molar flow rate of $\dot{N}_{air}$. The tubular construction of each cell causes the air to first enter the cell through the air supply tube and then reverse its direction to enter the cathode chamber. The cathode air serves as the source of oxygen for the fuel cell.

IV. SYSTEM MODEL

The essential dynamics of the SOFC system in Fig.1 are modeled using fundamental solid volume and gas control volume models. The control development presented in this paper is primarily based on mass balance equations of the reformer and the fuel cell. Hence we omit the heat transfer and thermodynamic models and present the relevant mass balance equations for the sake of brevity. The mass balance equation for individual species is constructed as follows,

$$N_g \dot{\mathcal{X}}_{j,g} = \dot{\zeta}_{in}\mathcal{X}_{j,in} - \dot{\zeta}_{ex}\mathcal{X}_{j,g} + \mathcal{R}_{j,g},\ j = 1, 2, \cdots, 7 \quad (1)$$

where specific values of subscripts j, $j = 1, 2, \cdots, 7$, correspond to the species CH_4, CO, CO_2, H_2, H_2O, N_2, and O_2 respectively. From Eq.(1), we additionally have

$$\begin{array}{c} \sum_{j=1}^{7} \mathcal{X}_{j,in} = \sum_{j=1}^{7} \mathcal{X}_{j,g} = 1 \ \Rightarrow\ \sum_{j=1}^{7} \dot{\mathcal{X}}_{j,g} = 0 \\ \Rightarrow\ \dot{\zeta}_{ex} = \dot{\zeta}_{in} + \sum_{j=1}^{7} \mathcal{R}_{j,g} \end{array} \quad (2)$$

Flow is assumed to be governed by a nominal pressure drop across each module, as in [9] and [11], and hence pressure variations are neglected.

A. Reformer Model

For steam reforming of methane we consider a packed-bed tubular reformer with nickel-alumina catalyst [7]. A schematic diagram of the steam reformer is shown in Fig.2. The exhaust, reformate and recirculated flows are modeled

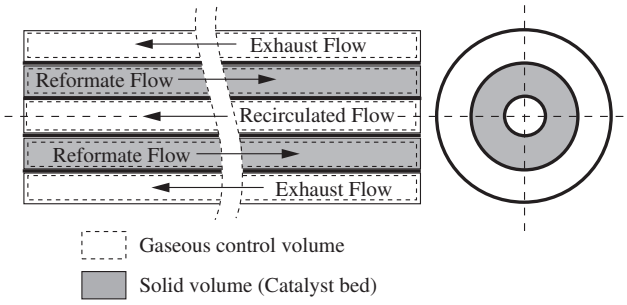

Fig. 2. Schematic diagram of tubular steam reformer

using gas control volumes and the catalyst bed is modeled as a solid volume. The three main reactions that simultaneously occur during steam reforming of methane are, [14]:

$$\begin{array}{lrcl} \text{(I)} & CH_4 + H_2O & \leftrightarrow & CO + 3H_2 \\ \text{(II)} & CO + H_2O & \leftrightarrow & CO_2 + H_2 \\ \text{(III)} & CH_4 + 2H_2O & \leftrightarrow & CO_2 + 4H_2 \end{array} \quad (3)$$

From Fig.1, the mass balance equations for CH_4, CO, CO_2, H_2 and H_2O can be written using Eq.(1) as follows:

$$\begin{array}{rcl} N_r\dot{\mathcal{X}}_{1,r} &=& k\dot{N}_o\mathcal{X}_{1,a} - \dot{N}_{in}\mathcal{X}_{1,r} + \mathcal{R}_{1,r} + \dot{N}_f \\ N_r\dot{\mathcal{X}}_{2,r} &=& k\dot{N}_o\mathcal{X}_{2,a} - \dot{N}_{in}\mathcal{X}_{2,r} + \mathcal{R}_{2,r} \\ N_r\dot{\mathcal{X}}_{3,r} &=& k\dot{N}_o\mathcal{X}_{3,a} - \dot{N}_{in}\mathcal{X}_{3,r} + \mathcal{R}_{3,r} \\ N_r\dot{\mathcal{X}}_{4,r} &=& k\dot{N}_o\mathcal{X}_{4,a} - \dot{N}_{in}\mathcal{X}_{4,r} + \mathcal{R}_{4,r} \\ N_r\dot{\mathcal{X}}_{5,r} &=& k\dot{N}_o\mathcal{X}_{5,a} - \dot{N}_{in}\mathcal{X}_{5,r} + \mathcal{R}_{5,r} \end{array} \quad (4)$$

where $N_r = P_rV_r/R_uT_r$. Note that the reformer inlet and exit flows shown in Fig.1 do not contain O_2 and N_2. Hence $\mathcal{X}_{6,r} = \mathcal{X}_{7,r} = 0$. From Eq.(3), we express $\mathcal{R}_{j,r}$, $j = 1, 2, \cdots, 5$, in terms of the reaction rates r_I, r_{II} and r_{III} as follows

$$\mathbf{R}_r = \mathbf{G}\,\mathbf{r},\ \mathbf{G} = \begin{bmatrix} -1 & 0 & -1 \\ 1 & -1 & 0 \\ 0 & 1 & 1 \\ 3 & 1 & 4 \\ -1 & -1 & -2 \end{bmatrix},\ \mathbf{R}_r = \begin{bmatrix} \mathcal{R}_{1,r} \\ \mathcal{R}_{2,r} \\ \mathcal{R}_{3,r} \\ \mathcal{R}_{4,r} \\ \mathcal{R}_{5,r} \end{bmatrix} \quad (5)$$

$\mathbf{r} = [r_I, r_{II}, r_{III}]^T$. Since $\mathbf{G}$ has a rank of 2, therefore there are only two independent reaction rates among $\mathcal{R}_{j,r}$, $j = 1, 2, \cdots, 5$. Considering the rate of formation of CH_4 and CO in the reformer to be independent, we can write

$$\begin{array}{rcl} \mathcal{R}_{3,r} &=& -\mathcal{R}_{1,r} - \mathcal{R}_{2,r} \\ \mathcal{R}_{4,r} &=& -4\mathcal{R}_{1,r} - \mathcal{R}_{2,r} \\ \mathcal{R}_{5,r} &=& 2\mathcal{R}_{1,r} + \mathcal{R}_{2,r} \end{array} \quad (6)$$

and rewrite Eq.(4) as follows:

$$\begin{array}{rcl} N_r\dot{\mathcal{X}}_{1,r} &=& k\dot{N}_o\mathcal{X}_{1,a} - \dot{N}_{in}\mathcal{X}_{1,r} + \mathcal{R}_{1,r} + \dot{N}_f \\ N_r\dot{\mathcal{X}}_{2,r} &=& k\dot{N}_o\mathcal{X}_{2,a} - \dot{N}_{in}\mathcal{X}_{2,r} + \mathcal{R}_{2,r} \\ N_r\dot{\mathcal{X}}_{3,r} &=& k\dot{N}_o\mathcal{X}_{3,a} - \dot{N}_{in}\mathcal{X}_{3,r} - \mathcal{R}_{1,r} - \mathcal{R}_{2,r} \\ N_r\dot{\mathcal{X}}_{4,r} &=& k\dot{N}_o\mathcal{X}_{4,a} - \dot{N}_{in}\mathcal{X}_{4,r} - 4\mathcal{R}_{1,r} - \mathcal{R}_{2,r} \\ N_r\dot{\mathcal{X}}_{5,r} &=& k\dot{N}_o\mathcal{X}_{5,a} - \dot{N}_{in}\mathcal{X}_{5,r} + 2\mathcal{R}_{1,r} + \mathcal{R}_{2,r} \end{array} \quad (7)$$

From Eqs.(2) and (7) we deduce

$$\dot{N}_{in} = k\dot{N}_o + \dot{N}_f + \sum_{j=1}^{7}\mathcal{R}_{j,r} \Rightarrow \dot{N}_{in} = k\dot{N}_o + \dot{N}_f - 2\mathcal{R}_{1,r} \quad (8)$$

B. SOFC Model

We assume our system to be comprised of $\mathcal{N}_{cell}$ tubular Solid Oxide Fuel Cells, connected in series. A schematic diagram of an individual cell is shown in Fig.3. The anode, cathode and air flows are modeled using gas control volumes. The air feed tube and the electrolyte are modeled as solid volumes. The following chemical and electro-chemical reactions occur simultaneously in the anode control volume:

$$\begin{array}{lrcl} \text{(I)} & CH_4 + H_2O & \leftrightarrow & CO + 3H_2 \\ \text{(II)} & CO + H_2O & \leftrightarrow & CO_2 + H_2 \\ \text{(III)} & CH_4 + 2H_2O & \leftrightarrow & CO_2 + 4H_2 \\ \text{(IV)} & H_2 + O^{2-} & \rightarrow & H_2O + 2e \end{array} \quad (9)$$

Steam reforming, represented by reactions I, II and III, occur in the anode due to high temperatures and the presence of nickel catalyst. The primary electrochemical process is steam generation from H_2, described by reaction IV. Simultaneous electrochemical conversion of CO to CO_2 in the anode is also possible. However, this electro-chemical reaction is ignored since its reaction rate is much slower in presence of reactions II and IV, as indicated in [2] and references therein.

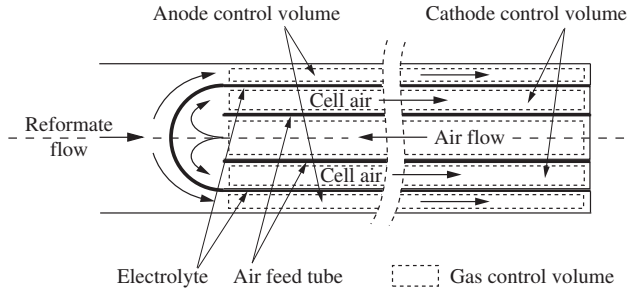

Fig. 3. Schematic diagram of tubular SOFC

From Fig.1 and Eq.(1), the mass balance equations for CH_4, CO, CO_2, H_2 and H_2O can be written as

$$\begin{array}{rcl} N_a\dot{\mathcal{X}}_{1,a} &=& -\dot{N}_o\mathcal{X}_{1,a} + \dot{N}_{in}\mathcal{X}_{1,r} + \mathcal{R}_{1,a} \\ N_a\dot{\mathcal{X}}_{2,a} &=& -\dot{N}_o\mathcal{X}_{2,a} + \dot{N}_{in}\mathcal{X}_{2,r} + \mathcal{R}_{2,a} \\ N_a\dot{\mathcal{X}}_{3,a} &=& -\dot{N}_o\mathcal{X}_{3,a} + \dot{N}_{in}\mathcal{X}_{3,r} + \mathcal{R}_{3,a} \\ N_a\dot{\mathcal{X}}_{4,a} &=& -\dot{N}_o\mathcal{X}_{4,a} + \dot{N}_{in}\mathcal{X}_{4,r} + \mathcal{R}_{4,a} - r_e \\ N_a\dot{\mathcal{X}}_{5,a} &=& -\dot{N}_o\mathcal{X}_{5,a} + \dot{N}_{in}\mathcal{X}_{5,r} + \mathcal{R}_{5,a} + r_e \end{array} \quad (10)$$

where $N_a = P_aV_a/R_uT_a$ and r_e is the rate of electrochemical reaction given by

$$r_e = \frac{i\mathcal{N}_{cell}}{nF} \quad (11)$$

Since current i can be measured, the rate of electrochemical reaction r_e is considered known. As with the reformate control volume, the anode inlet and exit flows do not contain O_2 and N_2. Therefore, $\mathcal{X}_{6,a} = \mathcal{X}_{7,a} = 0$. From Eq.(9), we express $\mathcal{R}_{j,a}$, $j = 1, 2, \cdots, 5$, in terms of the reaction rates r_I, r_{II} and r_{III} as follows

$$\mathbf{R}_a = \mathbf{G}\,\mathbf{r} + r_e\,[0\ \ 0\ \ 0\ \ -1\ \ 1]^T$$

where $\mathbf{R}_a = [\mathcal{R}_{1,a}\ \mathcal{R}_{2,a}\ \mathcal{R}_{3,a}\ \mathcal{R}_{4,a}\ \mathcal{R}_{5,a}]^T$, and $\mathbf{G}$ and $\mathbf{r}$ are given in Eq.(5). Since $\mathbf{G}$ has a rank of 2 and r_e is known, therefore there are only two independent reaction rates among $\mathcal{R}_{j,a}$, $j = 1, 2, \cdots, 5$. Considering $\mathcal{R}_{1,a}$ and $\mathcal{R}_{2,a}$ to be independent, we can write

$$\begin{array}{rcl} \mathcal{R}_{3,a} &=& -\mathcal{R}_{1,a} - \mathcal{R}_{2,a}, \\ \mathcal{R}_{4,a} &=& -4\mathcal{R}_{1,a} - \mathcal{R}_{2,a} - r_e, \\ \mathcal{R}_{5,a} &=& 2\mathcal{R}_{1,a} + \mathcal{R}_{2,a} + r_e \end{array} \quad (12)$$

and rewrite Eq.(10) as

$$\begin{array}{rcl} N_a\dot{\mathcal{X}}_{1,a} &=& -\dot{N}_o\mathcal{X}_{1,a} + \dot{N}_{in}\mathcal{X}_{1,r} + \mathcal{R}_{1,a} \\ N_a\dot{\mathcal{X}}_{2,a} &=& -\dot{N}_o\mathcal{X}_{2,a} + \dot{N}_{in}\mathcal{X}_{2,r} + \mathcal{R}_{2,a} \\ N_a\dot{\mathcal{X}}_{3,a} &=& -\dot{N}_o\mathcal{X}_{3,a} + \dot{N}_{in}\mathcal{X}_{3,r} - \mathcal{R}_{1,a} - \mathcal{R}_{2,a} \\ N_a\dot{\mathcal{X}}_{4,a} &=& -\dot{N}_o\mathcal{X}_{4,a} + \dot{N}_{in}\mathcal{X}_{4,r} - 4\mathcal{R}_{1,a} - \mathcal{R}_{2,a} - r_e \\ N_a\dot{\mathcal{X}}_{5,a} &=& -\dot{N}_o\mathcal{X}_{5,a} + \dot{N}_{in}\mathcal{X}_{5,r} + 2\mathcal{R}_{1,a} + \mathcal{R}_{2,a} + r_e \end{array} \quad (13)$$

From Eqs.(2) and (13) we deduce that

$$\dot{N}_o = \dot{N}_{in} + \sum_{j=1}^{7} \mathcal{R}_{j,a} \quad \Rightarrow \quad \dot{N}_o = \dot{N}_{in} - 2\mathcal{R}_{1,a} \qquad (14)$$

V. PROBLEM STATEMENT AND PRIOR DESIGN

The observer design problem statement is as follows: Given that temperatures and pressures can be sensed in the reformer and anode volumes, and given that the fuel cell current and voltage can be measured, design an observer for estimation of rates of steam reformation reactions, molar flow rates and species concentrations using a minimum number of concentration sensors.

We summarize our prior observer design [3] which used four concentration sensors. The sensing requirement is that any two species of the gas mixture must be sensed at the reformer and anode exits. We state the equations for a sample observer design where CH_4 and CO concentrations are sensed in the reformer and anode volumes, i.e., measurements of $\mathcal{X}_{1,r}$, $\mathcal{X}_{1,a}$, $\mathcal{X}_{2,r}$, $\mathcal{X}_{2,a}$ are assumed to be available. Note that this choice is arbitrary and similar observers can be designed by sensing any two of CH_4, CO, CO_2, H_2, and H_2O at the reformer and anode exits. The variables to be estimated are $\dot{N}_{in}$, $\dot{N}_o$, $\mathcal{R}_{2,r}$, $\mathcal{R}_{2,a}$, $\mathcal{X}_{i,r}$, $\mathcal{X}_{i,a}$, $i = 1, 2, \cdots, 5$. Their estimates are denoted by $\hat{\dot{N}}_{in}$, $\hat{\dot{N}}_o$, $\hat{\mathcal{R}}_{2,r}$, $\hat{\mathcal{R}}_{2,a}$, $\hat{\mathcal{X}}_{i,r}$, $\hat{\mathcal{X}}_{i,a}$, $i = 1, 2, \cdots, 5$. Based on Eqs.(7), (8), (13), and (14), the following observer equations are proposed

$$\begin{aligned}
N_r\dot{\hat{\mathcal{X}}}_{1,r} &= k\hat{\dot{N}}_o\left(\hat{\mathcal{X}}_{1,a}+0.5\right) - \hat{\dot{N}}_{in}\left(\hat{\mathcal{X}}_{1,r}+0.5\right) \\
&\quad +\mathcal{L}_{1,r}\,\mathcal{E}_{1,r} + 1.5\dot{N}_f \\
N_a\dot{\hat{\mathcal{X}}}_{1,a} &= -\hat{\dot{N}}_o\left(\hat{\mathcal{X}}_{1,a}+0.5\right) + \hat{\dot{N}}_{in}\left(\hat{\mathcal{X}}_{1,r}+0.5\right) \\
&\quad +\mathcal{L}_{1,a}\,\mathcal{E}_{1,a} \\
N_r\dot{\hat{\mathcal{X}}}_{2,r} &= k\hat{\dot{N}}_o\hat{\mathcal{X}}_{2,a} - \hat{\dot{N}}_{in}\hat{\mathcal{X}}_{2,r} + \hat{\mathcal{R}}_{2,r} + \mathcal{L}_{2,r}\,\mathcal{E}_{2,r} \\
N_a\dot{\hat{\mathcal{X}}}_{2,a} &= -\hat{\dot{N}}_o\hat{\mathcal{X}}_{2,a} + \hat{\dot{N}}_{in}\hat{\mathcal{X}}_{2,r} + \hat{\mathcal{R}}_{2,a} + \mathcal{L}_{2,a}\,\mathcal{E}_{2,a} \\
N_r\dot{\hat{\mathcal{X}}}_{3,r} &= k\hat{\dot{N}}_o\left(\hat{\mathcal{X}}_{3,a}-0.5\right) - \hat{\dot{N}}_{in}\left(\hat{\mathcal{X}}_{3,r}-0.5\right) \\
&\quad -0.5\dot{N}_f - \hat{\mathcal{R}}_{2,r} \\
N_a\dot{\hat{\mathcal{X}}}_{3,a} &= -\hat{\dot{N}}_o\left(\hat{\mathcal{X}}_{3,a}-0.5\right) + \hat{\dot{N}}_{in}\left(\hat{\mathcal{X}}_{3,r}-0.5\right) \\
&\quad -\hat{\mathcal{R}}_{2,a} \\
N_r\dot{\hat{\mathcal{X}}}_{4,r} &= k\hat{\dot{N}}_o\left(\hat{\mathcal{X}}_{4,a}-2\right) - \hat{\dot{N}}_{in}\left(\hat{\mathcal{X}}_{4,r}-2\right) \\
&\quad -2\dot{N}_f - \hat{\mathcal{R}}_{2,r} \\
N_a\dot{\hat{\mathcal{X}}}_{4,a} &= -\hat{\dot{N}}_o\left(\hat{\mathcal{X}}_{4,a}-2\right) + \hat{\dot{N}}_{in}\left(\hat{\mathcal{X}}_{4,r}-2\right) \\
&\quad -\hat{\mathcal{R}}_{2,a} - i\mathcal{N}_{cell}/nF \\
N_r\dot{\hat{\mathcal{X}}}_{5,r} &= k\hat{\dot{N}}_o\left(\hat{\mathcal{X}}_{5,a}+1\right) - \hat{\dot{N}}_{in}\left(\hat{\mathcal{X}}_{5,r}-1\right) \\
&\quad +\dot{N}_f + \hat{\mathcal{R}}_{2,r} \\
N_a\dot{\hat{\mathcal{X}}}_{5,a} &= -\hat{\dot{N}}_o\left(\hat{\mathcal{X}}_{5,a}+1\right) + \hat{\dot{N}}_{in}\left(\hat{\mathcal{X}}_{5,r}+1\right) \\
&\quad +\hat{\mathcal{R}}_{2,a} + i\mathcal{N}_{cell}/nF
\end{aligned}$$

along with the following adaptation laws

$$\begin{aligned}
\dot{\hat{\dot{N}}}_{in} &= \gamma_1\left[\left(\mathcal{E}_{1,a}-\mathcal{E}_{1,r}\right)\left(\hat{\mathcal{X}}_{1,r}+0.5\right)\right. \\
&\quad \left.+\left(\mathcal{E}_{2,a}-\mathcal{E}_{2,r}\right)\hat{\mathcal{X}}_{2,r}\right] \\
\dot{\hat{\dot{N}}}_{o} &= \gamma_2\left[\left(k\mathcal{E}_{1,r}-\mathcal{E}_{1,a}\right)\left(\hat{\mathcal{X}}_{1,a}+0.5\right)\right. \\
&\quad \left.+\left(k\mathcal{E}_{2,r}-\mathcal{E}_{2,a}\right)\hat{\mathcal{X}}_{2,a}\right] \\
\dot{\hat{\mathcal{R}}}_{2,r} &= \gamma_3\,\mathcal{E}_{2,r} \\
\dot{\hat{\mathcal{R}}}_{2,a} &= \gamma_4\,\mathcal{E}_{2,a}
\end{aligned}$$

where, $\gamma_1, \gamma_2, \gamma_3, \gamma_4 > 0$, $\mathcal{L}_{1,r}, \mathcal{L}_{1,a}, \mathcal{L}_{2,r}, \mathcal{L}_{2,a} > 0$, $\mathcal{E}_{1,r} = \mathcal{X}_{1,r} - \hat{\mathcal{X}}_{1,r}$, $\mathcal{E}_{1,a} = \mathcal{X}_{1,a} - \hat{\mathcal{X}}_{1,a}$, $\mathcal{E}_{2,r} = \mathcal{X}_{2,r} - \hat{\mathcal{X}}_{2,r}$, and $\mathcal{E}_{2,a} = \mathcal{X}_{2,a} - \hat{\mathcal{X}}_{2,a}$. This nonlinear observer guarantees uniform asymptotic stability of the observer error dynamics.

VI. DESIGN USING CELL VOLTAGE MEASUREMENT

A. Observer Design

In the previous section we have outlined an observer design procedure that uses four concentration sensors. In this section we propose an observer design that uses cell voltage measurement and three concentration sensors, reducing the number of required concentration sensors by one. The three required concentration sensors are a steam and a hydrogen sensor at the reformer outlet and a steam sensor at the anode outlet. Hence, in addition to cell voltage V_{cell}, the measurements of $\mathcal{X}_{4,r}$, $\mathcal{X}_{5,r}$, and $\mathcal{X}_{5,a}$ are assumed to be available. The observer equations are

$$\begin{aligned}
N_r\dot{\hat{\mathcal{X}}}_{1,r} &= k\hat{\dot{N}}_o\left(\hat{\mathcal{X}}_{1,a}+0.5\right) - \hat{\dot{N}}_{in}\left(\hat{\mathcal{X}}_{1,r}+0.5\right) \\
&\quad +1.5\dot{N}_f + \eta_{1,r} \\
N_a\dot{\hat{\mathcal{X}}}_{1,a} &= -\hat{\dot{N}}_o\left(\hat{\mathcal{X}}_{1,a}+0.5\right) + \hat{\dot{N}}_{in}\left(\hat{\mathcal{X}}_{1,r}+0.5\right) \\
&\quad +\eta_{1,a} \\
N_r\dot{\hat{\mathcal{X}}}_{2,r} &= k\hat{\dot{N}}_o\hat{\mathcal{X}}_{2,a} - \hat{\dot{N}}_{in}\hat{\mathcal{X}}_{2,r} + \hat{\mathcal{R}}_{2,r} + \eta_{2,r} \\
N_a\dot{\hat{\mathcal{X}}}_{2,a} &= -\hat{\dot{N}}_o\hat{\mathcal{X}}_{2,a} + \hat{\dot{N}}_{in}\hat{\mathcal{X}}_{2,r} + \hat{\mathcal{R}}_{2,a} + \eta_{2,a} \\
N_r\dot{\hat{\mathcal{X}}}_{3,r} &= k\hat{\dot{N}}_o\left(\hat{\mathcal{X}}_{3,a}-0.5\right) - \hat{\dot{N}}_{in}\left(\hat{\mathcal{X}}_{3,r}-0.5\right) \\
&\quad -0.5\dot{N}_f - \hat{\mathcal{R}}_{2,r} + \eta_{3,r} \\
N_a\dot{\hat{\mathcal{X}}}_{3,a} &= -\hat{\dot{N}}_o\left(\hat{\mathcal{X}}_{3,a}-0.5\right) + \hat{\dot{N}}_{in}\left(\hat{\mathcal{X}}_{3,r}-0.5\right) \\
&\quad -\hat{\mathcal{R}}_{2,a} + \eta_{3,a} \\
N_r\dot{\hat{\mathcal{X}}}_{4,r} &= k\hat{\dot{N}}_o\left(\hat{\mathcal{X}}_{4,a}-2\right) - \hat{\dot{N}}_{in}\left(\hat{\mathcal{X}}_{4,r}-2\right) \\
&\quad -2\dot{N}_f - \hat{\mathcal{R}}_{2,r} + \mathcal{L}_{4,r}\,\mathcal{E}_{4,r} + \eta_{4,r} \\
N_a\dot{\hat{\mathcal{X}}}_{4,a} &= -\hat{\dot{N}}_o\left(\hat{\mathcal{X}}_{4,a}-2\right) + \hat{\dot{N}}_{in}\left(\hat{\mathcal{X}}_{4,r}-2\right) \\
&\quad -\hat{\mathcal{R}}_{2,a} - i\mathcal{N}_{cell}/nF + \eta_{4,a} \\
N_r\dot{\hat{\mathcal{X}}}_{5,r} &= k\hat{\dot{N}}_o\left(\hat{\mathcal{X}}_{5,a}+1\right) - \hat{\dot{N}}_{in}\left(\hat{\mathcal{X}}_{5,r}+1\right) \\
&\quad +\dot{N}_f + \hat{\mathcal{R}}_{2,r} + \mathcal{L}_{5,r}\,\mathcal{E}_{5,r} + \eta_{5,r} \\
N_a\dot{\hat{\mathcal{X}}}_{5,a} &= -\hat{\dot{N}}_o\left(\hat{\mathcal{X}}_{5,a}+1\right) + \hat{\dot{N}}_{in}\left(\hat{\mathcal{X}}_{5,r}+1\right) \\
&\quad +\hat{\mathcal{R}}_{2,a} + i\mathcal{N}_{cell}/nF + \mathcal{L}_{5,a}\,\mathcal{E}_{5,a} + \eta_{5,a}
\end{aligned} \qquad (15)$$

with the following adaptation laws

$$\begin{aligned}
\dot{\hat{N}}_{in} &= \gamma_1 \left[(\mathcal{E}_{4,r}/N_r - \xi_{4,a}/N_a) \left(2 - \hat{\mathcal{X}}_{4,r}\right) \right. \\
&\quad \left. + (\mathcal{E}_{5,a}/N_a - \mathcal{E}_{5,r}/N_r) \left(\hat{\mathcal{X}}_{5,r} + 1\right) \right] + \eta_{p1} \\
\dot{\hat{N}}_{o} &= \gamma_2 \left[(k\mathcal{E}_{4,r}/N_r - \xi_{4,a}/N_a) \left(\hat{\mathcal{X}}_{4,a} - 2\right) \right. \\
&\quad \left. + (k\mathcal{E}_{5,r}/N_r - \mathcal{E}_{5,a}/N_a) \left(\hat{\mathcal{X}}_{5,a} + 1\right) \right] + \eta_{p2} \\
\dot{\hat{\mathcal{R}}}_{2,r} &= \gamma_3 \left[\mathcal{E}_{5,r}/N_r - \mathcal{E}_{4,r}/N_r \right] + \eta_{p3} \\
\dot{\hat{\mathcal{R}}}_{2,a} &= \gamma_4 \left[\mathcal{E}_{5,a}/N_a - \xi_{4,a}/N_a \right] + \eta_{p4}
\end{aligned} \tag{16}$$

where,

$$\mathcal{E}_{4,r} = \mathcal{X}_{4,r} - \hat{\mathcal{X}}_{4,r},\ \mathcal{E}_{5,r} = \mathcal{X}_{5,r} - \hat{\mathcal{X}}_{5,r},\ \mathcal{E}_{5,a} = \mathcal{X}_{5,a} - \hat{\mathcal{X}}_{5,a} \tag{17}$$

and $\mathcal{L}_{4,r}$, $\mathcal{L}_{5,r}$, $\mathcal{L}_{5,a}$, γ_1, γ_2, γ_3 and γ_4 are positive constants. In Eq.(16), $\xi_{4,a}$ is given by

$$\xi_{4,a} = \bar{\mathcal{X}}_{4,a} - \hat{\mathcal{X}}_{4,a} \tag{18}$$

where $\bar{\mathcal{X}}_{4,a}$ is an estimate of $\mathcal{X}_{4,a}$ obtained dynamically using the cell voltage and measurement $\mathcal{X}_{5,a}$, given as follows:

$$\begin{aligned}
\dot{\hat{\mathcal{X}}}_{4,a} &= k_o \left[V_{cell} - \hat{V}_{cell} + qT_a \ln(\mathcal{X}_{5,a}) - qT_a \ln(\hat{\mathcal{X}}_{5,a}) \right] \\
&\quad + \bar{\eta}_{4,a},\ k_o > 0
\end{aligned} \tag{19}$$

The cell voltage V_{cell} of the SOFC system is expressed as follows:

$$V_{cell} = f_1(T_a, T_c, i) + \frac{R_u T_a}{nF} \ln \left(p_{H_2} p_{O_2}^{1/2} / p_{H_2O} \right) \tag{20}$$

Since $p_{H_2} = P_a \mathcal{X}_{4,a}$, $p_{O_2} = P_c \mathcal{X}_{7,c}$, and $p_{H_2O} = P_a \mathcal{X}_{5,a}$, we can express Eq.(20) as

$$V_{cell} = f_2(T_a, T_c, P_c, i, \mathcal{X}_{7,c}) + qT_a \left[\ln(\mathcal{X}_{4,a}) - \ln(\mathcal{X}_{5,a}) \right] \tag{21}$$

where $f_2 = f_1 + 0.5 \left(R_u T_a / nF\right) \ln \left(P_c \mathcal{X}_{7,c}\right)$ and $q = (R_u/nF)$. The estimate $\hat{V}_c$ is given by

$$\hat{V}_{cell} = f_2(T_a, T_c, P_c, i, \mathcal{X}_{7,c}) + qT_a \left[\ln(\bar{\mathcal{X}}_{4,a}) - \ln(\hat{\mathcal{X}}_{5,a}) \right] \tag{22}$$

In Eqs.(15), (16), and (19), the terms $\eta_{1,r}$, $\eta_{1,a}$, $\eta_{2,r}$, $\eta_{2,a}$, $\eta_{3,r}$, $\eta_{3,a}$, $\eta_{4,r}$, $\eta_{4,a}$, $\bar{\eta}_{4,a}$, $\eta_{5,r}$, $\eta_{5,a}$, η_{p1}, η_{p2}, η_{p3}, and η_{p4} are included to provide upper and lower bounds on state and parameter estimates and prevent integrator wind-up. For instance, $\eta_{1,r}$ and η_{p1} are designed as

$$\eta_{1,r} = \begin{cases} -g_{1,r} & \text{if} \quad \left(\hat{\mathcal{X}}_{1,r} \geq 1 \text{ and } g_{1,r} > 0\right) \\ & \text{or} \quad \left(\hat{\mathcal{X}}_{1,r} \leq 0 \text{ and } g_{1,r} < 0\right) \\ 0 & \text{otherwise} \end{cases}$$

$$g_{1,r} = k_o \dot{\hat{N}}_o \left(\hat{\mathcal{X}}_{1,a} + 0.5\right) - \dot{\hat{N}}_{in} \left(\hat{\mathcal{X}}_{1,r} + 0.5\right) + 1.5 \dot{N}_f \tag{23}$$

$$\eta_{p1} = \begin{cases} -g_{p1} & \text{if} \quad \left(\dot{\hat{N}}_{in} \geq \dot{N}_{in,max} \text{ and } g_{p1} > 0\right) \\ & \text{or} \quad \left(\dot{\hat{N}}_{in} \leq \dot{N}_{in,min} \text{ and } g_{p1} < 0\right) \\ 0 & \text{otherwise} \end{cases}$$

$$g_{p1} = \gamma_1 \Big[(\mathcal{E}_{4,r} - \xi_{4,a}) \Big(2 - \hat{\mathcal{X}}_{4,r}\Big) + (\mathcal{E}_{5,a} - \mathcal{E}_{5,r}) \Big(\hat{\mathcal{X}}_{5,r} + 1\Big) \Big] \tag{24}$$

The upper and lower bounds on the concentration estimates are 1 and 0 respectively. The bounds on the estimates of $\dot{\hat{N}}_{in}$, $\dot{\hat{N}}_o$, $\dot{\hat{\mathcal{R}}}_{2,r}$ and $\dot{\hat{\mathcal{R}}}_{2,a}$ are dependent on the specific application.

B. Boundedness and Convergence

We first prove that $\bar{\mathcal{E}}_{4,a} = \mathcal{X}_{4,a} - \bar{\mathcal{X}}_{4,a}$ is ultimately bounded. From Eqs.(19), (21) and (22), we have

$$\dot{\bar{\mathcal{E}}}_{4,a} = -k_o\, q\, T_a \left[ln(\mathcal{X}_{4,a}) - ln(\bar{\mathcal{X}}_{4,a}) \right] + \dot{\mathcal{X}}_{4,a} - \bar{\eta}_{4,a}$$

Taking $V = 0.5 \bar{\mathcal{E}}_{4,a}^2$ as a Lyapunov function candidate and noting from the *Mean Value Theorem* that $\left[ln(\mathcal{X}_{4,a}) - ln(\bar{\mathcal{X}}_{4,a}) \right] = \lambda\, \bar{\mathcal{E}}_{4,a},\ \lambda \geq 1$, we have

$$\begin{aligned}
\dot{V} &= -k_o\, q\, T_a\, \bar{\mathcal{E}}_{4,a} \left[ln(\mathcal{X}_{4,a}) - ln(\bar{\mathcal{X}}_{4,a}) \right] \\
&\quad + \bar{\mathcal{E}}_{4,a}\, \dot{\mathcal{X}}_{4,a} - \bar{\mathcal{E}}_{4,a} \bar{\eta}_{4,a} \\
&\leq -k_o\, q\, T_a\, \bar{\mathcal{E}}_{4,a}^2 + |\bar{\mathcal{E}}_{4,a}|\, |\dot{\mathcal{X}}_{4,a}| \\
&= -k_o\, q\, T_a\, (1 - \theta_1) \bar{\mathcal{E}}_{4,a}^2 - k_o\, q\, T_a\, \theta_1 \bar{\mathcal{E}}_{4,a}^2 \\
&\quad + |\bar{\mathcal{E}}_{4,a}|\ \sup \left(|\dot{\mathcal{X}}_{4,a}| \right) \\
&< -k_o\, q\, T_a\, (1 - \theta_1) |\bar{\mathcal{E}}_{4,a}|^2 \\
&\quad \forall \quad |\bar{\mathcal{E}}_{4,a}| > \mu_1,\ \mu_1 \triangleq \tfrac{\sup \left(|\dot{\mathcal{X}}_{4,a}| \right)}{k_o\, q\, T_a\, \theta_1}
\end{aligned} \tag{25}$$

where $0 < \theta_1 < 1$. Note that in Eq.(25), the term $\bar{\mathcal{E}}_{4,a} \bar{\eta}_{4,a} \geq 0$. This can be inferred from Eqs.(23) and (24). If $\bar{\mathcal{X}}_{4,a} \geq 1$ and $\bar{g}_{4,a} > 0$, then $\bar{\mathcal{E}}_{4,a} \leq 0$ and $\bar{\eta}_{4,a} < 0$. Similarly, if $\bar{\mathcal{X}}_{4,a} \leq 0$ and $\bar{g}_{4,a} < 0$, then $\bar{\mathcal{E}}_{4,a} \geq 0$ and $\bar{\eta}_{4,a} > 0$. Otherwise, $\bar{\eta}_{4,a} = 0$. Also note that in Eq.(25), $\sup |\dot{\mathcal{X}}_{4,a}|$ can be obtained from the range of operating conditions. It can be easily shown that $\bar{\mathcal{E}}_{4,a}$ is uniformly ultimately bounded with an ultimate bound of μ_1. Hence, by choosing k_o to be large, causing $\bar{\mathcal{X}}_{4,a}$ in Eq.(19) to be singularly perturbed, $\bar{\mathcal{E}}_{4,a}$ can be brought arbitrarily close to zero.

We next prove the ultimate boundedness of the state estimation errors $\mathcal{E}_{4,r}$, $\mathcal{E}_{4,a}$, $\mathcal{E}_{5,r}$, and $\mathcal{E}_{5,a}$. The variables $\mathcal{E}_{4,r}$, $\mathcal{E}_{5,r}$, and $\mathcal{E}_{5,a}$ are defined in Eq.(17) and

$$\mathcal{E}_{4,a} = \mathcal{X}_{4,a} - \hat{\mathcal{X}}_{4,a} \tag{26}$$

Consider the following Lyapunov function candidate

$$\begin{aligned}
V &= \tfrac{1}{2} \left[\mathcal{E}_{4,r}^2 + \mathcal{E}_{4,a}^2 + \mathcal{E}_{5,r}^2 + \mathcal{E}_{5,a}^2 \right. \\
&\quad \left. + \tfrac{1}{\gamma_1} \mathcal{E}_{\dot{N}_{in}}^2 + \tfrac{1}{\gamma_2} \mathcal{E}_{\dot{N}_o}^2 + \tfrac{1}{\gamma_3} \mathcal{E}_{\dot{\mathcal{R}}_{2,r}}^2 + \tfrac{1}{\gamma_4} \mathcal{E}_{\dot{\mathcal{R}}_{2,a}}^2 \right]
\end{aligned}$$

where

$$\begin{aligned}
\mathcal{E}_{\dot{N}_{in}} &= \dot{N}_{in} - \dot{\hat{N}}_{in}, \quad \mathcal{E}_{\dot{N}_o} = \dot{N}_o - \dot{\hat{N}}_o, \\
\mathcal{E}_{\dot{\mathcal{R}}_{2,r}} &= \dot{\mathcal{R}}_{2,r} - \dot{\hat{\mathcal{R}}}_{2,r}, \quad \mathcal{E}_{\dot{\mathcal{R}}_{2,a}} = \dot{\mathcal{R}}_{2,a} - \dot{\hat{\mathcal{R}}}_{2,a} \\
\dot{\mathcal{E}}_{\dot{N}_{in}} &= -\ddot{\hat{N}}_{in}, \dot{\mathcal{E}}_{\dot{N}_o} = -\ddot{\hat{N}}_o, \dot{\mathcal{E}}_{\dot{\mathcal{R}}_{2,r}} = -\ddot{\hat{\mathcal{R}}}_{2,r}, \dot{\mathcal{E}}_{\dot{\mathcal{R}}_{2,a}} = -\ddot{\hat{\mathcal{R}}}_{2,a}
\end{aligned} \tag{27}$$

From Eqs.(15), (16), (18), (26), and (27), the derivative of V along the system trajectories can be expressed as

$$\begin{aligned}
\dot{V} = &-(\mathcal{L}_{4,r} + \dot{N}_{in}) \mathcal{E}_{4,r}^2 / N_r + (k\, \dot{N}_o / N_r + \dot{N}_{in} / N_a) \mathcal{E}_{4,r}\, \mathcal{E}_{4,a} \\
&- \dot{N}_o \mathcal{E}_{4,a}^2 / N_a - (\mathcal{L}_{5,r} + \dot{N}_{in}) \mathcal{E}_{5,r}^2 / N_r \\
&+ (k\, \dot{N}_o / N_r + \dot{N}_{in} / N_a) \mathcal{E}_{5,r}\, \mathcal{E}_{5,a} - (\mathcal{L}_{5,a} + \dot{N}_o) \mathcal{E}_{5,a}^2 / N_a \\
&+ \bar{\mathcal{E}}_{4,a} \left[(2 - \hat{\mathcal{X}}_{4,a}) \mathcal{E}_{\dot{N}_o} + (\hat{\mathcal{X}}_{4,r} - 2) \mathcal{E}_{\dot{N}_{in}} - \mathcal{E}_{\dot{\mathcal{R}}_{2,a}} \right] / N_a \\
&- \eta_{4,r} \mathcal{E}_{4,r} - \eta_{4,a} \mathcal{E}_{4,a} - \eta_{5,r} \mathcal{E}_{5,r} - \eta_{5,a} \mathcal{E}_{5,a} \\
&- \eta_{p1} \mathcal{E}_{\dot{N}_{in}} - \eta_{p2} \mathcal{E}_{\dot{N}_o} - \eta_{p3} \mathcal{E}_{\dot{\mathcal{R}}_{2,r}} - \eta_{p4} \mathcal{E}_{\dot{\mathcal{R}}_{2,a}}
\end{aligned}$$

From Eqs.(23) and (24) and the discussion after Eq.(25) we can show that

$$\eta_{4,r}\mathcal{E}_{4,r} \geq 0,\ \eta_{4,a}\mathcal{E}_{4,a} \geq 0,\ \eta_{5,r}\mathcal{E}_{5,r} \geq 0,\ \ \eta_{5,a}\mathcal{E}_{5,a} \geq 0$$
$$\eta_{p1}\mathcal{E}_{\dot{N}_{in}} \geq 0,\ \eta_{p2}\mathcal{E}_{\dot{N}_o} \geq 0,\ \eta_{p3}\mathcal{E}_{\mathcal{R}_{2,r}} \geq 0,\ \eta_{p4}\mathcal{E}_{\mathcal{R}_{2,a}} \geq 0$$

Hence,

$$\begin{aligned}\dot{V} \leq & -\mathbf{E}_4^T\,\mathbf{Q}_4\,\mathbf{E}_4 - \mathbf{E}_5^T\,\mathbf{Q}_5\,\mathbf{E}_5 \\ & +\bar{\mathcal{E}}_{4,a}\Big[(2-\hat{\mathcal{X}}_{4,a})\mathcal{E}_{\dot{N}_o}+(\hat{\mathcal{X}}_{4,r}-2)\mathcal{E}_{\dot{N}_{in}}-\mathcal{E}_{\mathcal{R}_{2,a}}\Big]/N_a\end{aligned} \tag{28}$$

where

$$\mathbf{E}_4 = [\mathcal{E}_{4,r}\mathcal{E}_{4,a}]^T, \quad \mathbf{E}_5 = [\mathcal{E}_{5,r}\mathcal{E}_{5,a}]^T$$

$$\mathbf{Q}_4 = \begin{bmatrix} \frac{(\mathcal{L}_{4,r}+\dot{N}_{in})}{N_r} & -0.5(\frac{k\,\dot{N}_o}{N_r}+\frac{\dot{N}_{in}}{N_a}) \\ -0.5(\frac{k\,\dot{N}_o}{N_r}+\frac{\dot{N}_{in}}{N_a}) & \frac{\dot{N}_o}{N_a} \end{bmatrix}$$

$$\mathbf{Q}_5 = \begin{bmatrix} \frac{(\mathcal{L}_{5,r}+\dot{N}_{in})}{N_r} & -0.5(\frac{k\,\dot{N}_o}{N_r}+\frac{\dot{N}_{in}}{N_a}) \\ -0.5(\frac{k\,\dot{N}_o}{N_r}+\frac{\dot{N}_{in}}{N_a}) & \frac{(\mathcal{L}_{5,a}+\dot{N}_o)}{N_a} \end{bmatrix}$$

The molar flow rates $\dot{N}_{in}$ and $\dot{N}_o$ are positive and bounded, and $0 < k < 1$. Furthermore, in the fuel cell $\dot{N}_o > \dot{N}_{in}$. This is because in the anode internal steam reforming produces more product molecules from fewer reactant molecules and the electrochemical reaction conserves the number of molecules. Also, the molar contents $N_r = P_r\,V_r/R_u\,T_r$ and $N_a = P_a\,V_a/R_u\,T_a$ are positive with bounds dependent on the range of operating conditions. Hence, proper choice of the observer gains $\mathcal{L}_{4,r}$, $\mathcal{L}_{5,r}$, and $\mathcal{L}_{5,a}$ will ensure positive definiteness of $\mathbf{Q}_4$ and $\mathbf{Q}_5$. It can be shown that $\mathbf{Q}_4$ will be positive definite if

$$\begin{aligned}\mathcal{L}_{4,r} &> \tfrac{1}{\dot{N}_o}\left[\tfrac{1}{4}(k\,\dot{N}_o\,N_a+\dot{N}_{in}\,N_r)^2-\dot{N}_o\,\dot{N}_{in}\right] \\ \Rightarrow \mathcal{L}_{4,r} &\geq [\max(\sup(N_r),\sup(N_a))]^2\,\sup\left(\dot{N}_o\right)\end{aligned} \tag{29}$$

With $\mathcal{L}_{5,r} = \mathcal{L}_{5,a} = \mathcal{L}_5$, we can show that $\mathbf{Q}_5$ will be positive definite if

$$\begin{aligned}\left(\dot{N}_{in}+\mathcal{L}_5\right)\left(\dot{N}_o+\mathcal{L}_5\right) &> \tfrac{1}{4}(k\,\dot{N}_o\,N_a+\dot{N}_{in}\,N_r)^2 \\ \Rightarrow \mathcal{L}_5 &\geq \max(\sup(N_r),\sup(N_a))\sup\left(\dot{N}_o\right)\end{aligned} \tag{30}$$

Thus, using the *Rayleigh-Ritz inequality*, we have

$$\begin{aligned}\mathbf{E}_4^T\,\mathbf{Q}_4\,\mathbf{E}_4 &\geq \inf(\lambda_{4,min})\|\mathbf{E}_4\|^2, \\ \mathbf{E}_5^T\,\mathbf{Q}_5\,\mathbf{E}_5 &\geq \inf(\lambda_{5,min})\|\mathbf{E}_5\|^2\end{aligned}$$

where $\lambda_{4,min}$ and $\lambda_{5,min}$ are the smaller eigenvalues of $\mathbf{Q}_4$ and $\mathbf{Q}_5$ respectively. Hence,

$$\begin{aligned}&\mathbf{E}_4^T\,\mathbf{Q}_4\,\mathbf{E}_4 + \mathbf{E}_5^T\,\mathbf{Q}_5\,\mathbf{E}_5 \geq \bar{\lambda}\,\|\mathbf{E}_{4,5}\|^2, \\ &\bar{\lambda} \triangleq \min\left(\inf(\lambda_{4,min}),\,\inf(\lambda_{5,min})\right), \quad \bar{\lambda} > 0\end{aligned} \tag{31}$$

where $\mathbf{E}_{4,5} = [\mathbf{E}_4\ \mathbf{E}_5]^T = [\mathcal{E}_{4,r}\ \mathcal{E}_{4,a}\ \mathcal{E}_{5,r}\ \mathcal{E}_{5,a}]^T$. Note that $\dot{N}_{in}$, $\dot{N}_o$ and $\mathcal{R}_{2,a}$ are bounded variables and their estimates, along with $\hat{\mathcal{X}}_{4,r}$, $\hat{\mathcal{X}}_{4,a}$, and N_a are also bounded by design (Eqs.(15) and (16)). Therefore, from Eqs.(28) and (31) we deduce

$$\begin{aligned}\dot{V} &\leq -\bar{\lambda}\,\|\mathbf{E}_{4,5}\|^2 + |\bar{\mathcal{E}}_{4,a}|\,h_{max} \\ &= -\bar{\lambda}\,(1-\theta_2)\,\|\mathbf{E}_{4,5}\|^2 - \bar{\lambda}\,\theta_2\,\|\mathbf{E}_{4,5}\|^2 + |\bar{\mathcal{E}}_{4,a}|\,h_{max} \\ &< -\bar{\lambda}(1-\theta_2)\,\|\mathbf{E}_{4,5}\|^2, \\ &\quad \forall\ \|\mathbf{E}_{4,5}\| > \mu_2,\ \mu_2 \triangleq \sqrt{\mu_1\,h_{max}/\bar{\lambda}\,\theta_2}\end{aligned} \tag{32}$$

where, $0 < \theta_2 < 1$ and

$$h_{max} = \sup\Big(\Big[(2-\hat{\mathcal{X}}_{4,a})\mathcal{E}_{\dot{N}_o}+(\hat{\mathcal{X}}_{4,r}-2)\mathcal{E}_{\dot{N}_{in}}-\mathcal{E}_{\mathcal{R}_{2,a}}\Big]/N_a\Big)$$

Thus $\|\mathbf{E}_{4,5}\|$ is ultimately bounded with an ultimate bound of μ_2. Furthermore, from the definitions of μ_1 and $\bar{\lambda}$ in Eqs.(25) and (31), we infer that μ_2 can be made arbirarily small by choosing large observer gains k_o and $\bar{\lambda}$.

Next we show that $\hat{\dot{N}}_{in}$, $\hat{\dot{N}}_o$, $\hat{\mathcal{R}}_{2,r}$ and $\hat{\mathcal{R}}_{2,a}$ converge to their true values with small bounded errors. Since μ_2 can be made arbitrarily small, for every $t_0 \geq 0$ there exists $T \geq 0$ such that $\eta_{4,r} = \eta_{4,a} = \eta_{5,r} = \eta_{5,a} = 0$ for $t > t_0 + T$. Therefore, for sufficiently large t_0, the state equation for $\mathbf{E}_{4,5}$ can be written as

$$\dot{\mathbf{E}}_{4,5} = \mathbf{A}_{4,5}\,\mathbf{E}_{4,5} + \mathbf{B}_{4,5}\,\mathbf{E}_p \tag{33}$$

where $\mathbf{E}_p = [\mathcal{E}_{\dot{N}_{in}}\ \mathcal{E}_{\dot{N}_o}\ \mathcal{E}_{\mathcal{R}_{2,r}}\ \mathcal{E}_{\mathcal{R}_{2,a}}]^T$,

$$\mathbf{A}_{4,5} = \begin{bmatrix} -\frac{(\mathcal{L}_{4,r}+\dot{N}_{in})}{N_r} & \frac{k\dot{N}_o}{Nr} & 0 & 0 \\ \frac{\dot{N}_{in}}{N_a} & -\frac{\dot{N}_o}{N_a} & 0 & 0 \\ 0 & 0 & -\frac{(\mathcal{L}_{5,r}+\dot{N}_{in})}{N_r} & \frac{k\dot{N}_o}{Nr} \\ 0 & 0 & \frac{\dot{N}_{in}}{N_a} & -\frac{(\mathcal{L}_{5,r}+\dot{N}_o)}{N_a} \end{bmatrix}$$

$$\mathbf{B}_{4,5} = \begin{bmatrix} -\frac{(\hat{\mathcal{X}}_{4,r}-2)}{N_r} & \frac{k(\hat{\mathcal{X}}_{4,a}-2)}{N_r} & -\frac{1}{N_r} & 0 \\ \frac{(\hat{\mathcal{X}}_{4,r}-2)}{N_a} & -\frac{(\hat{\mathcal{X}}_{4,a}-2)}{N_a} & 0 & -\frac{1}{N_a} \\ -\frac{(1+\hat{\mathcal{X}}_{5,r})}{N_r} & \frac{k(1+\hat{\mathcal{X}}_{5,a})}{N_r} & \frac{1}{N_r} & 0 \\ \frac{(1+\hat{\mathcal{X}}_{5,r})}{N_a} & -\frac{(1+\hat{\mathcal{X}}_{5,a})}{N_a} & 0 & \frac{1}{N_a} \end{bmatrix} \tag{34}$$

From Eq.(33), we have

$$\ddot{\mathbf{E}}_{4,5} = \mathbf{A}_{4,5}\,\dot{\mathbf{E}}_{4,5} + \dot{\mathbf{A}}_{4,5}\,\mathbf{E}_{4,5} + \dot{\mathbf{B}}_{4,5}\,\mathbf{E}_p + \mathbf{B}_{4,5}\,\dot{\mathbf{E}}_p \tag{35}$$

In Eq.(35), $\|\mathbf{A}_{4,5}\|$ and $\|\dot{\mathbf{A}}_{4,5}\|$ are bounded with bounds on N_r, N_a, $\dot{N}_r$, $\dot{N}_a$, $\dot{N}_{in}$, $\dot{N}_o$, $\ddot{N}_{in}$ and $\ddot{N}_o$ governed by the operating conditions of the fuel cell. $\|\mathbf{E}_{4,5}\|$ was shown to be bounded with an ultimate bound of μ_2. $\|\mathbf{B}_{4,5}\|$ and $\|\dot{\mathbf{B}}_{4,5}\|$ are bounded due to the observer design in Eq.(15). $\|\mathbf{E}_p\|$ and $\|\dot{\mathbf{E}}_p\|$ are also bounded by virtue of the design of the adaptation laws in Eq.(16). Finally, $\|\dot{\mathbf{E}}_{4,5}\|$ is bounded as inferred from Eq.(33) and the foregoing discussion. Hence $\|\ddot{\mathbf{E}}_{4,5}\|$ is bounded. We can show that

$$\begin{aligned}&\|\mathbf{E}_{4,5}\| \leq \mu_2,\ \|\ddot{\mathbf{E}}_{4,5}\| \leq \mu_3,\ \mu_2,\ \mu_3 > 0 \\ &\Rightarrow \quad \|\dot{\mathbf{E}}_{4,5}\| \leq \sqrt{2\mu_2\,\mu_3}\end{aligned} \tag{36}$$

The result can be proven through elementary geometry and is omitted here for brevity. From Eqs.(33) and (35), we deduce that

$$\|\ddot{\mathbf{E}}_{4,5}\| \leq c_1\,\mu_2 + c_2, \quad \Rightarrow \quad \mu_3 = c_1\,\mu_2 + c_2 \tag{37}$$

where c_1 and c_2 are fixed positive constants given by

$$c_1 = \sup(\|\mathbf{A}_{4,5}\|^2 + \|\dot{\mathbf{A}}_{4,5}\|),$$
$$c_2 = \sup(\left[\|\mathbf{A}_{4,5}\|\,\|\mathbf{B}_{4,5}\| + \|\dot{\mathbf{B}}_{4,5}\|\right]\,\|\mathbf{E}_p\| + \|\mathbf{B}_{4,5}\|\,\|\dot{\mathbf{E}}_p\|)$$

From Eqs.(36) and (37), we conclude that as $\mu_2 \rightarrow 0$ with large values of the observer gains k_o and $\bar{\lambda}$, both $\|\mathbf{E}_{4,5}\|$ and $\|\dot{\mathbf{E}}_{4,5}\|$ approach ultimate bounds that are arbitrarily close to zero. From Eq.(34) we infer that since $\|\mathbf{E}_{4,5}\| \leq \mu_2$, for all feasible operating conditions of the solid oxide fuel cell, $\mathbf{B}_{4,5}$ will be non-singular and therefore from Eq.(33) we have

$$\begin{aligned} \mathbf{E}_p &= \mathbf{B}_{4,5}^{-1}\left[\dot{\mathbf{E}}_{4,5} - \mathbf{A}_{4,5}\,\mathbf{E}_{4,5}\right] \\ \Rightarrow \|\mathbf{E}_p\| &\leq \|\mathbf{B}_{4,5}^{-1}\|\,\left[\sqrt{2\mu_2\,(c_1\,\mu_2 + c_2)} + \|\mathbf{A}_{4,5}\|\,\mu_2\right] \end{aligned} \tag{38}$$

From Eq.(38) it is clear that as $\mu_2 \rightarrow 0$ so will $\|\mathbf{E}_p\|$ and this implies convergence of $\hat{\dot{N}}_{in}$, $\hat{\dot{N}}_o$, $\hat{\mathcal{R}}_{2,r}$ and $\hat{\mathcal{R}}_{2,a}$ to their true values with small bounded errors.

Finally we show that the remaining state estimates, $\hat{\mathcal{X}}_{1,r}$, $\hat{\mathcal{X}}_{2,r}$, $\hat{\mathcal{X}}_{3,r}$, $\hat{\mathcal{X}}_{1,a}$, $\hat{\mathcal{X}}_{2,a}$, and $\hat{\mathcal{X}}_{3,a}$, are ultimately bounded around their true values with small errors. We prove this by establishing the ISS (*input-to-state stability*) property [10] of $\mathcal{E}_{1,r}$, $\mathcal{E}_{1,a}$, $\mathcal{E}_{2,r}$, $\mathcal{E}_{2,a}$, $\mathcal{E}_{3,r}$, and $\mathcal{E}_{3,a}$, where

$$\begin{aligned} \mathcal{E}_{1,r} &= \mathcal{X}_{1,r} - \hat{\mathcal{X}}_{1,r}, \quad \mathcal{E}_{1,a} = \mathcal{X}_{1,a} - \hat{\mathcal{X}}_{1,a}, \\ \mathcal{E}_{2,r} &= \mathcal{X}_{2,r} - \hat{\mathcal{X}}_{2,r}, \quad \mathcal{E}_{2,a} = \mathcal{X}_{2,a} - \hat{\mathcal{X}}_{2,a}, \\ \mathcal{E}_{3,r} &= \mathcal{X}_{3,r} - \hat{\mathcal{X}}_{3,r}, \quad \mathcal{E}_{3,a} = \mathcal{X}_{3,a} - \hat{\mathcal{X}}_{3,a} \end{aligned}$$

Consider the state equation of $\mathbf{E}_3$ which is given as

$$\dot{\mathbf{E}}_3 = \mathbf{Q}_3\,\mathbf{E}_3 + \mathbf{B}_3\,\mathbf{E}_p \tag{39}$$

where,

$$\mathbf{E}_3 = [\mathcal{E}_{3,r}\mathcal{E}_{3,a}]^T, \quad \mathbf{Q}_3 = \begin{bmatrix} \frac{\dot{N}_{in}}{N_r} & -\frac{k\,\dot{N}_o}{N_r} \\ -\frac{\dot{N}_{in}}{N_a} & \frac{\dot{N}_o}{N_a} \end{bmatrix} \tag{40}$$

and

$$\mathbf{B}_3 = \begin{bmatrix} -\frac{(\hat{\mathcal{X}}_{3,r}-0.5)}{N_r} & \frac{k(\hat{\mathcal{X}}_{3,a}-0.5)}{N_r} & -\frac{1}{N_r} & 0 \\ \frac{(\hat{\mathcal{X}}_{3,r}-0.5)}{N_a} & -\frac{(\hat{\mathcal{X}}_{3,a}-0.5)}{N_a} & 0 & -\frac{1}{N_a} \end{bmatrix}$$

Considering $\mathbf{B}_3\,\mathbf{E}_p$ to be the input in Eq.(39), the origin of the unforced system

$$\dot{\mathbf{E}}_3 = \mathbf{Q}_3\,\mathbf{E}_3$$

is globally exponentially stable since $\mathbf{Q}_3$ and $\dot{\mathbf{Q}}_3$ are bounded and the pointwise eigenvalues of $\mathbf{Q}_3$ are negative and real [12]. Hence, the system in Eq.(39) is ISS. Therefore $\|\mathbf{E}_3\|$ is ultimately bounded by a class $\mathcal{K}$ function of $\sup(\|\mathbf{B}_3\|)\sup(\|\mathbf{E}_p\|)$. From Eq.(38) it is clear that as $\mu_2 \rightarrow 0$ so will $\|\mathbf{E}_p\|$. Thus, as $\|\mathbf{E}_p\| \rightarrow 0$ so will $\|\mathbf{E}_3\|$, confirming that the convergence of $\hat{\dot{N}}_{in}$, $\hat{\dot{N}}_o$, $\hat{\mathcal{R}}_{2,r}$ and $\hat{\mathcal{R}}_{2,a}$ to their true values will lead to correct estimation of $\mathcal{X}_{3,r}$, and $\mathcal{X}_{3,a}$. Similar conclusions can be drawn for $\mathcal{X}_{1,r}$, $\mathcal{X}_{2,a}$, $\mathcal{X}_{2,r}$, and $\mathcal{X}_{2,a}$ by performing similar analysis as above for the state equations of $\mathbf{E}_1 = [\mathcal{E}_{1,r}\mathcal{E}_{1,a}]^T$ and $\mathbf{E}_2 = [\mathcal{E}_{2,r}\mathcal{E}_{2,a}]^T$.

C. Simulations

We provide simulation results to demonstrate the performance of the voltage based observer design presented in the foregoing sections. The observer was tested on the comprehensive fuel cell model that captures the details of heat and mass transfer, chemical kinetics and electrochemistry. We performed an open-loop simulation of the plant model in conjunction with the observer. For the simulation, we chose $\dot{N}_f = 0.01$moles/s, $\dot{N}_{air} = 0.1$moles/s, and $k = 0.75$. The current demand was changed in steps as given below

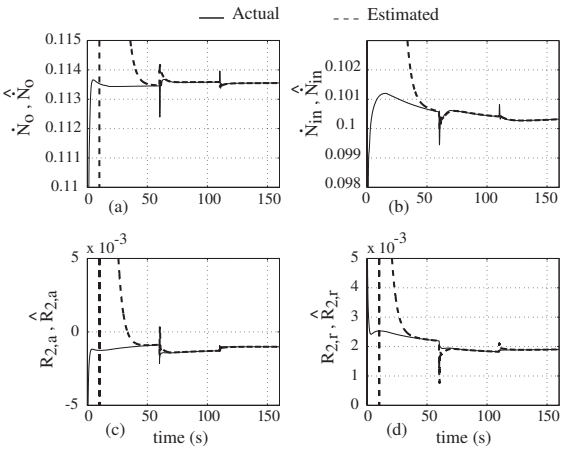

Fig. 4. $\dot{N}_{in}$, $\dot{N}_o$, $\mathcal{R}_{2,r}$, and $\mathcal{R}_{2,a}$ and their estimates

$$i = \begin{cases} 65 & \text{for} \quad 0 \leq t \leq 60 \\ 70 & \text{for} \quad 60 < t \leq 110 \\ 68 & \text{for} \quad 110 < t \end{cases}$$

The values of the observer gains are chosen as $k_o = 10$, $\mathcal{L}_{4,r} = \mathcal{L}_5 = 1$, and $\gamma_1 = \gamma_2 = \gamma_3 = \gamma_4 = 250$. The estimation algorithm was switched on at $t = 10$s and was left active for the rest of the simulation. The estimates $\hat{\dot{N}}_{in}$, $\hat{\dot{N}}_o$, $\hat{\mathcal{R}}_{2,r}$, and $\hat{\mathcal{R}}_{2,a}$, along with their model-generated actual values are plotted in Fig.4. The accuracy of these estimates is important since it directly determines the estimation accuracy

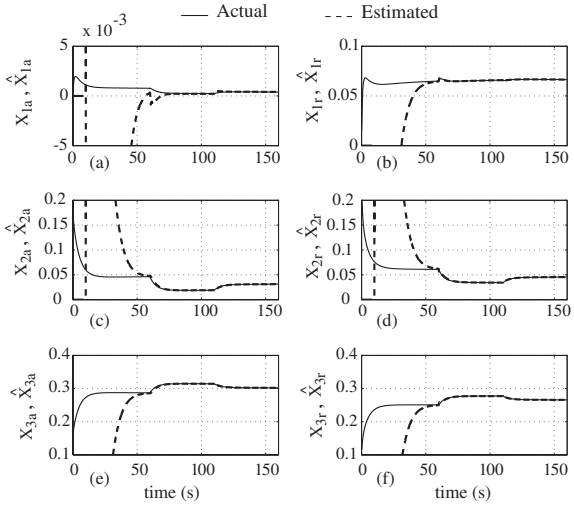

Fig. 5. CH_4, CO, CO_2 mole fractions and their estimates

of CH_4, CO and CO_2 concentrations, which are shown in Fig.5. The corresponding plots of H_2 and H_2O are omitted for conciseness.

We have outlined an observer design procedure that uses three concentration sensors and cell voltage measurement. The number of concentration sensors can be further reduced by one if measurements of the net molar flow rates at the exit of the reformer and anode, i.e. if $\dot{N}_{in}$ and $\dot{N}_o$, are available. The development of the observer equations are left to the reader for the sake of brevity.

VII. CONCLUSION

We have presented an observer design for species concentration estimation in recirculation based solid oxide fuel cell systems. In this design we do not assume the knowledge of the rates of reforming reactions. Instead, they are treated as variables that are dynamically estimated in conjunction with dynamic concentration estimation. The proposed observer desin is based on cell voltage measurement. We show that this observer guarantees ultimate boundedness of state and parameter estimation errors. The error bounds can made arbitrarily small through proper choice of observer gains. Simulation results are provided in support of our proposed observer design.

REFERENCES

[1] M. Arcak, H. Gorgun, L. M. Pedersen, and S. Varigonda. A nonlinear observer design for fuel cell hydrogen estimation. *IEEE TRansactions on Control Systems Technology*, 12(1):101–110, 2004.

[2] R. Bove, P Lunghi, and N. M. Sammes. Sofc mathematic model for systems simulations - part 2: Definition of an analytical model. *International Journal of Hydrogen Energy*, 30:189–200, 2005.

[3] T. Das and R. Mukherjee. Observer design for a steam reformer based solid oxide fuel cell system with anode recirculation. *ASME, IMECE, Seattle, WA*, 2007.

[4] D. Dochain. State observers for processes with uncertain kinetics. *International Journal of Control*, 76(15):1483–1492, 2003.

[5] M. L. Ferrari, A. Traverso, L. Magistri, and A. F. Massardo. Influence of anodic recirculation transient behavior on the sofc hybrid system performance. *Journal of Power Sources*, 149:22–32, 2005.

[6] H. Gorgun, M. Arcak, S. Varigonda, and S. A. Bortoff. Observer designs for fuel processing reactors in fuel cell power systems. *International Journal of Hydrogen Energy*, 30:447–457, 2005.

[7] F. P. Incropera and D. P. DeWitt. *Fundamentals of Heat and Mass Transfer*. John Wiley & Sons, Inc., fifth edition, 2002.

[8] N. M. Iyer and A. E. Farell. Design of a stable adaptive nonlinear observer for an exothermic stirred tank reactor. *Comp. Chem. Engg.*, 20(9):1141–1147, 1996.

[9] R. Kandepu, L. Imsland, B. A. Foss, C. Stiller, B. Thorud, and O. Bolland. Modeling and control of a sofc-gt-based autonomous power system. *Energy*, 32:406–417, 2007.

[10] H. K. Khalil. *Nonlin. Sys.* Prentice Hall, third edition, 2002.

[11] F. Mueller, J. Brouwer, F. Jabbari, and S. Samuelsen. Dynamic simulation of an integrated solid oxide fuel cell system including current-based fuel flow control. *ASME Journal of Fuel Cell Science and Technology*, 3:144–154, 2006.

[12] W. J. Rugh. *Lin. Sys. Th.* Prentice Hall, second edition, 1996.

[13] M. Soroush. Nonlinear state-observer design with application to reactors. *Chemical Engineering Science*, 52(3):387–404, 1997.

[14] J. Xu and G. F. Froment. Methane steam reforming, methanation and water-gas shift: I. intrinsic kinetics. *AIChE Journal*, 35(1):88–96, 1989.